# Mechanistic Investigation of Particle Size Effects in TEMPO-Mediated Radical Polymerization of Styrene in Aqueous Miniemulsion

**Per B. Zetterlund, Tadashi Nakamura, and Masayoshi Okubo***

*Department of Chemical Science and Engineering, Graduate School of Engineering, Kobe University, Kobe 657-8501, Japan*

*Received June 4, 2007; Revised Manuscript Received August 1, 2007*

ABSTRACT: Particle size effects in the diameter range 70−200 nm in 2,2,6,6-tetramethylpiperidinyl-1-oxy (TEMPO)-mediated radical polymerization of styrene in aqueous miniemulsion at 125 °C using sodium dodecylbenzenesulfonate as surfactant have been studied. Extensive investigations, including modeling and simulations of the polymerization, indicate that a significant fraction of free TEMPO is unable to participate in deactivation reactions if the particles are sufficiently small. The results are in support of our previously proposed interface effect [Nakamura, T.; Zetterlund, P. B.; Okubo, M. *Macromol. Rapid Commun.* **2006**, *27*, 2014−2018], according to which some fraction of the free TEMPO is located/adsorbed at the interface, thus reducing the effective TEMPO concentration in the organic phase.

## Introduction

Controlled/living radical polymerization (CLRP) has brought about a renaissance in the field of radical polymerization over the past 15 years. It is now possible to prepare a wide range of polymers of predefined molecular weights (MW), low polydispersities, and various complex architectures by free radical means.[1,2] The three most well-known techniques of CLRP are nitroxide-mediated polymerization (NMP),[3,4] atom transfer radical polymerization (ATRP),[5,6] and reversible addition−fragmentation chain transfer (RAFT) polymerization.[7] The present contribution is concerned with NMP using the nitroxide 2,2,6,6-tetramethylpiperidinyl-1-oxy (TEMPO), where control/livingness is achieved as a result of reversible capping of propagating radicals by TEMPO.

A major focus of recent work in CLRP is the implementation in aqueous dispersed systems.[8−11] In the case of NMP, early attempts at ab initio emulsion polymerizations met with limited success, mainly because of problems associated with nucleation and nitroxide partitioning.[12−14] Very recently, Charleux and coworkers successfully developed a true ab initio emulsion NMP system that relies on self-assembly of an in situ formed poly(sodium acrylate)-based amphiphilic diblock copolymer using the versatile nitroxide *N-tert*-butyl-*N*-[1-diethylphosphono(2,2-dimethylpropyl)] (SG1).[15,16] Not surprisingly, NMP has been more straightforward to implement in miniemulsion than ab initio emulsion because the complex nucleation step is avoided, and nitroxide transport through the aqueous phase is not a concern.[17−30]

In general, conventional (nonliving) radical polymerization in dispersed systems is more complex than homogeneous systems due to various mechanistic aspects that are unique to dispersed systems, such as entry/exit and compartmentalization.[31] The situation is even more complex in the case of CLRP in dispersed systems. For example, in NMP, the extent of nitroxide partitioning to the aqueous phase may influence the polymerization,[8,9,21,32] and for sufficiently small particles, the rate of deactivation may increase due to the confined space effect[33,34] (reaction between propagating radical and nitroxide occurring rapidly in a confined space). Ideally, one would like to exploit such characteristics to improve features such as the control/livingness or the polymerization rate ($R_p$) relative to the corresponding homogeneous system. Examples include the prospect of improving the control/livingness in NMP[33,34] and ATRP[35] in dispersed systems by exploiting the confined space effect on deactivation by use of sufficiently small particles as well as optimization of control/livingness and $R_p$ by exploitation of nitroxide partitioning to the aqueous phase.[21]

We have reported in a recent communication that the particle size exerts a very significant influence on $R_p$ and the control/livingness in the TEMPO-mediated aqueous miniemulsion polymerization of styrene (S) using sodium dodecylbenzenesulfonate (SDBS; 4−8 wt % rel S, $[SDBS]_{aq}$ = 12−24 mM; 5% solids content) as surfactant at 125 °C.[30] The value of $R_p$ increased, and the control/livingness decreased, with decreasing particle diameter (number-average diameter ($d_n$) ≈ 70−170 nm). These results were rationalized by invoking an interface effect, according to which some fraction of TEMPO would be located near or be adsorbed at the interface between the aqueous and the organic phase. As a consequence, the effective TEMPO concentration in the particles would be reduced, which in turn leads to a reduction in deactivation rate. Cunningham et al.[36,37] reported that $R_p$ for the same system at 135 °C increased with increasing SDBS content (3.1−15.4 wt % rel S, $[SDBS]_{aq}$ = 20−100 mM; 20% solids content) for very similar volume-average particle diameters of ∼120 nm (i.e., faster than the corresponding bulk system). However, in sharp contrast with our findings, the control/livingness was not significantly affected. These authors proposed that SDBS may participate in the generation of radicals, thus leading to higher $R_p$.

The aim of the present study is to further investigate the mechanism of the pronounced effect of particle size on TEMPO-mediated aqueous miniemulsion polymerization of S using SDBS as surfactant at 125 °C. To this end, a range of specific miniemulsion polymerizations have been carried out in the presence of an excess of free TEMPO and also employing a polymeric analogue of TEMPO to exclude nitroxide partitioning to the aqueous phase. Moreover, the TEMPO concentration in the polymer particles has been measured by electron paramagnetic resonance (EPR) spectroscopy. Extensive modeling and

* Corresponding author. Tel and Fax: +81-(0)78-803-6161; e-mail: okubo@kobe-u.ac.jp.

10.1021/ma0712403 CCC: $37.00 
Published on Web 10/24/2007

**Scheme 1. Polymeric TEMPO Macroinitiator**

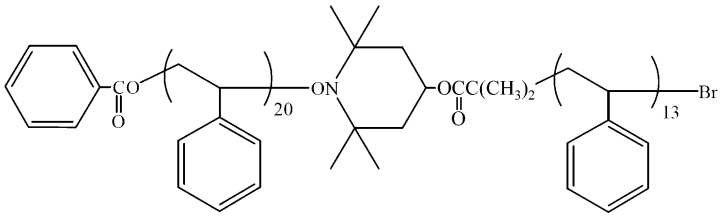

simulations of both $R_p$ and molecular weight distributions (MWD) have been carried out using the software PREDICI.[38] The results are discussed within the framework of the interface effect[30] proposed by us and the effect of SDBS proposed by Cunningham and co-workers.[37]

## Experimental Section

**Materials.** S was purified by distillation under reduced pressure in a nitrogen atmosphere. Deionized water with a specific resistance of $5 \times 10^6$ Ω·cm was distilled prior to use. Benzoyl peroxide (BPO) was recrystallized using chloroform/methanol. TEMPO, 4-hydroxy-TEMPO, 2-bromoisobutyl bromide, *N*,*N*′,*N*′,*N*″-pentamethyldiethylenetriamine (Aldrich), SDBS, toluene, methanol, *n*-hexadecane, CuBr, triethylamine (Nacalai Tesque Inc., Kyoto, Japan), anhydrous tetrahydrofuran (Wako Pure Chemicals), and 1-pyrenylmethyl methacrylate (Polysciences Inc.) were used as received.

**Preparation of PS-TEMPO Macroinitiator.** S (27 g), BPO (0.80 g, $3.31 \times 10^{-3}$ mol), and TEMPO (0.62 g, $3.97 \times 10^{-3}$ mol) were charged in a glass tube, degassed with several $N_2$ cycles, sealed off under vacuum, and heated at 125 °C for 4 h in an oil bath. The polymer was precipitated in excess methanol and reprecipitated four times using toluene/methanol and dried in a high-vacuum oven. Conversion = 19%, $M_n = 2100$, $M_w/M_n = 1.11$.

**Preparation of Polymeric TEMPO Macroinitiator.** Nitroxide-mediated polymerization of S in bulk was carried out by charging S (27 g), BPO (0.80 g, $3.31 \times 10^{-3}$ mol), and 4-hydroxy-TEMPO (0.68 g, $3.97 \times 10^{-3}$ mol) in a glass tube, which was subsequently degassed with several $N_2$ cycles, sealed off under vacuum, and heated at 125 °C for 4 h. The polymer was isolated by precipitation in methanol and purified by reprecipitation using toluene/methanol (conversion 22%, $M_n = 2400$, $M_w/M_n = 1.15$). The thus-obtained hydroxyl-terminated polymer was subsequently converted to α-bromoester-terminated polymer according to a literature procedure[39] by dropwise addition of 2-bromoisobutyl bromide to an anhydrous THF solution of hydroxyl-terminated polymer and triethylamine. The solution was left overnight at ambient temperature under a nitrogen atmosphere, and the polymer was purified by reprecipitation using toluene/methanol. Finally, chain extension of the α-bromoester-terminated polymer with S using ATRP was carried out by heating a mixture of S (13.6 g), CuBr (0.47 g, $3.33 \times 10^{-3}$ mol), and *N*,*N*,*N*′,*N*′,*N*″-pentamethyldiethylenetriamine (PMDETA; 0.57 g, $3.33 \times 10^{-3}$ mol) in a sealed glass tube under a nitrogen atmosphere at 70 °C until the mixture became homogeneous. The mixture was transferred to a glass ampule, degassed using several $N_2$/vacuum cycles, and subsequently a S (20 g) solution of the α-bromoester-terminated polymer (4.0 g, $1.67 \times 10^{-3}$ mol) was added under a $N_2$ atmosphere. The mixture was sealed off, shaken horizontally at 100 cycles/min at 70 °C, and polymerized to 7.2% conversion; $M_n = 3850$, $M_w/M_n = 1.09$ (Scheme 1).

Nitroxide-mediated polymerization of S (2 g) in bulk was carried out using the polymeric TEMPO macroinitiator (0.12 g, $3.12 \times 10^{-5}$ mol) to estimate its purity in terms of the number fraction of chains containing the alkoxyamine moiety. The macroinitiator and S were charged in a glass tube, degassed with several $N_2$ cycles, sealed off under vacuum, and heated at 125 °C for 5 h in an oil bath. The polymer was precipitated in excess methanol and dried in a high-vacuum oven. Conversion = 33%, $M_n = 16\,900$, $M_w/M_n = 1.27$. Transformation of the chain-extended MWD (not shown) to a number distribution[40] ($P(M)$ vs $M$) and integration of the low-MW peak (nonextended chains; MW < ∼6000 g/mol) relative to the overall distribution revealed that ∼88% of chains (by number) were living (in terms of the alkoxyamine moiety being intact).

**Scheme 2. 1-Pyrenylmethyl Methacrylate**

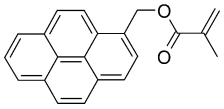

**Preparation of Fluorescence-Labeled TEMPO Macroinitiator.** A PS-TEMPO macroinitiator labeled[41] with a small amount of the fluorescence (FL) monomer 1-pyrenylmethyl methacrylate (Scheme 2) ($PS_{FL}$-TEMPO) was prepared by charging S (5 g, $4.81 \times 10^{-2}$ mol), BPO (137 mg, $5.66 \times 10^{-4}$ mol), TEMPO (105 mg, $6.72 \times 10^{-4}$ mol), and 1-pyrenylmethyl methacrylate (5.0 mg, $1.66 \times 10^{-5}$ mol) in a glass tube, followed by degassing with several $N_2$ cycles, sealing off under vacuum, and heating at 125 °C for 4 h in an oil bath. The polymerization mixture was subsequently diluted with toluene, and the polymer was precipitated in excess methanol and reprecipitated several times using toluene/methanol. The obtained polymer was dissolved in toluene followed by filtration to remove unreacted FL monomer and finally precipitated in methanol and dried in a high-vacuum oven. It is crucial that the obtained $PS_{FL}$-TEMPO is not contaminated with unreacted FL monomer because this would invalidate the subsequent FL-detector-based MWD analysis.[41] The absence of unreacted FL monomer was confirmed by GPC using FL detection. Conversion = 17%, $M_n = 2350$, $M_w/M_n = 1.10$.

The RI-detector response is proportional to polymer mass, but the FL-detector response is proportional to the concentration of FL units. Consequently, RI GPC data of polymer obtained by NMP in the absence of FL monomer using $PS_{FL}$-TEMPO cannot be directly compared with GPC data derived from the FL detector.[41] To enable direct quantitative comparison between the RI- and FL-detector derived MWDs, the "raw" MWD derived from the FL detector was converted to the equivalent RI-derived MWD by considering the mass ratio of the FL-labeled segment of the polymer to that of the nonlabeled segment. The correctness of this approach was verified by carrying out a solution (toluene) polymerization of S using $PS_{FL}$-TEMPO at 125 °C (data not shown). The raw GPC traces (detector response vs elution time) were different for the two detectors, as expected, but having followed the procedure outlined above, the $w(\log M)$ vs $\log M$ distributions[40] were close to identical. It should be noted however that an error is introduced when there is significant termination by combination.

**Polymerization Procedures.** Miniemulsion polymerizations with free TEMPO (5.0 wt % solids content): A solution of S (0.75 g), PS-TEMPO (35 mg, $1.67 \times 10^{-5}$ mol), *n*-hexadecane (60 mg; 8 wt % relative to S), and TEMPO (0.056, 0.14, or 0.52 mg) was mixed with an aqueous solution of SDBS (60 mg; 8 wt % relative to S). Emulsification was carried out using ultrasonication (Ultrasonic Homogenizer, Nissei, US-600T, 12 mm diameter tip, set at "Power 10") for 12 min at 0 °C in a 30 mL glass vial. The emulsions were subsequently transferred to glass ampules, degassed using several $N_2$/vacuum cycles, and sealed off under vacuum. Polymerizations were carried out at 125 °C shaking the ampules (∼4 mL/ampule) horizontally at 100 cycles/min.

The miniemulsion polymerizations using $PS_{FL}$-TEMPO were carried out in the same way (in the absence of free TEMPO), replacing PS-TEMPO with $PS_{FL}$-TEMPO (39 mg, $1.66 \times 10^{-5}$ mol).

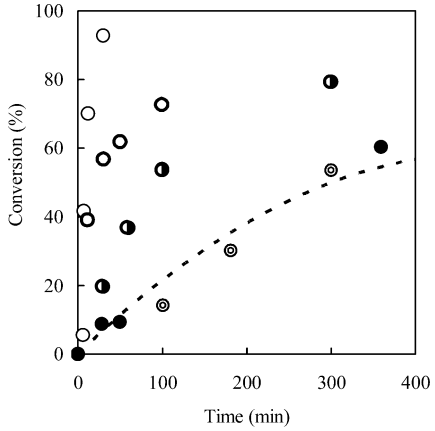


**Figure 1.** Conversion−time data for TEMPO-mediated miniemulsion polymerizations of S with $[PS\text{-}TEMPO]_0 = 0.02$ M at 125 °C using 4 (●; $d_n = 170$ nm and $d_w = 220$ nm) and 8 (◑; $d_n = 110$ nm and $d_w = 150$ nm; ○; $d_n = 70$ nm and $d_w = 90$ nm) wt % SDBS (relative to S), 8 wt % PVA (relative to S) (concentric circles; $d_n = 200$ nm and $d_w = 240$ nm), and using macroinitiator based on polymeric TEMPO (open circles with thick lines; $[macroinitiator]_0 = 0.02$ M) with 8 wt % SDBS ($d_n \approx 62$ nm and $d_w \approx 76$ nm). All polymerizations contained 8 wt % hexadecane (relative to S). The broken line is bulk at 125 °C from ref 52. All data except the polymeric TEMPO data are from ref 30.

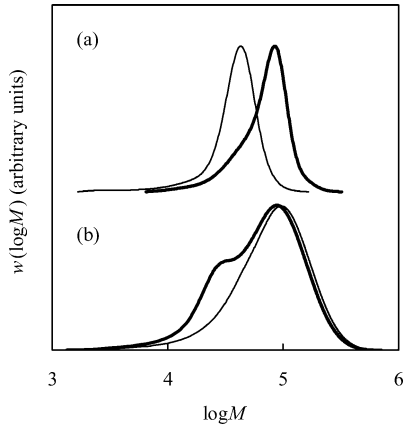


**Figure 2.** Chain extensions (thick lines) with S of the polymer (thin lines) obtained in TEMPO-mediated miniemulsion polymerizations by solution polymerization in toluene at 125 °C. Original polymer from miniemulsion polymerizations in Figure 1: (a) $d_n \approx 110$ nm at 79% conversion; chain extension: 200 min, 18% conversion; (b) $d_n \approx 70$ nm at 92% conversion; chain extension: 10 h, 16% conversion. See Experimental Section for details. The MWDs have been normalized to peak height.

The miniemulsion polymerizations using the macroinitiator based on polymeric TEMPO (Scheme 1) were also carried out as described above, except that PS-TEMPO was replaced with the polymeric TEMPO macroinitiator (64.0 mg), and no free TEMPO was added. The polymer obtained in the miniemulsion polymerizations was isolated by centrifugation (after addition of methanol) and drying.

Chain extensions in solution using polymer isolated from the TEMPO-mediated miniemulsion polymerizations detailed in our previous communication[30] were carried out to gain information on livingness for the polymerizations with (a) $d_n \approx 110$ nm at 79% conversion and (b) $d_n \approx 70$ nm at 92% conversion (see Figure 1): Solutions of (a) polymer (0.15 g) and S (1.06 g) in toluene (1.06 g) and (b) polymer (0.30 g) and S (0.34 g) in toluene (0.85 g) were degassed using several $N_2$/vacuum cycles and sealed off under vacuum. Polymerizations were carried out at 125 °C for 200 min (a) and 10 h (b) shaking the ampules horizontally at 80 cycles/min. Polymer was isolated for GPC measurements by precipitation in methanol. The value of $R_p$ was higher in chain extension (a) than (b) because the S concentration was higher in the former. (In TEMPO-mediated S polymerization in bulk/solution, $R_p$ is governed by the rate of thermal initiation of S (which depends on S concentration) and the termination rate and is independent of the PS-TEMPO concentration.[2])

**Measurements.** Particle size distributions were measured by dynamic light scattering (DLS-7000, Otsuka Electronics, Osaka, Japan) at the light scattering angle of 90° at room temperature after dilution to 10 ppm using S-saturated water. Number- ($d_n$) and weight-average ($d_w$) particle diameters were obtained using the Marquadt Analysis routine. The particle sizes remained approximately constant throughout the polymerizations (values given refer to average values).

S conversions were determined by gas chromatography (Shimadzu Corp., GC-18A) with helium as carrier gas, employing *N*,*N*-dimethylformamide as solvent and *p*-xylene as internal standard.

MWDs were measured by gel permeation chromatography (GPC) using two S/divinylbenzene gel columns (TOSOH Corp., TSKgel $GMH_{HR}$-H, 7.8 mm i.d × 30 cm, separation range per column: approximately $50-4 \times 10^8$ g/mol (exclusion limit)) using THF as eluent at 40 °C at a flow rate of 1.0 mL/min with refractive index detection (TOSOH RI-8020/21) and FL detection (JASCO FP-2020 Plus). The columns were calibrated with six standard PS samples ($1.05 \times 10^3-5.48 \times 10^6$, $M_w/M_n = 1.10-1.15$).

Interfacial tensions were measured by the pendant drop method using a Drop Master 500 (Kyowa Interface Science Co. Ltd.) instrument at room temperature. The accuracy of the measured interfacial tensions is of the order ±0.2 mN/m.

**Electron Paramagnetic Resonance (EPR) Spectroscopy.** In order to quantify the concentration of free TEMPO in the particles, EPR measurements were carried employing a JEOL (Japan) JES-T300 spectrometer using 5 mm o.d. quartz tubes at room temperature. EPR parameters: center field: 3350 G; microwave power: 0.5 mW; modulation amplitude: 5 G; number of scans: 1. Aqueous miniemulsion polymerization for EPR measurement was carried out as described above (no free TEMPO added; 8 wt % *n*-hexadecane and SDBS relative to S; $d_n \approx 110$ nm; 52% conversion in 100 min).

EPR sample preparation: The glass ampule containing the miniemulsion after polymerization was quenched in ice/water and subsequently placed in a freezer. Upon thawing, near complete coagulation had occurred. A known amount of the coagulum (which thus contains polymer, monomer, nitroxide, hexadecane, and some water) was collected and dried. The wt % of the organic phase in the coagulum before drying was calculated from the weight of the dried sample. The volume of the organic phase in the coagulum before drying was calculated on the basis of an assumed density of 1 g/cm$^3$. The actual EPR sample was subsequently prepared by dissolving a known amount of the coagulum (before drying) in toluene. The absolute concentration of TEMPO was obtained from the double integral of the EPR signal based on calibration with TEMPO. A linear calibration line was obtained by plotting the double integral of the EPR signal intensity vs the TEMPO concentration ($10^{-6}-10^{-3}$ M) using toluene solutions of TEMPO.

## Results and Discussion

**Polymerization Rate and Livingness.** Figure 1 shows conversion−time data of TEMPO-mediated polymerization of S in aqueous miniemulsion using SDBS as surfactant at 125 °C from our previous communication,[30] revealing how $R_p$ increased markedly with decreasing particle size. For particle diameters greater than ~170 nm, $R_p$ was the same as in bulk. The increase in $R_p$ was accompanied by some loss of control, as evidenced by the MWDs displayed in ref 30. In the present study, adverse effects also on the livingness were confirmed by chain extensions of the isolated polymer. The polymerization with intermediate $R_p$ ($d_n \approx 110$ nm; 79% conversion sample) exhibited partial livingness, as evident from the overall shift to higher MW (Figure 2a). However, a pronounced low-MW shoulder existed. Transformation of the chain extended MWD to a

number distribution[40] ($P(M)$ vs $M$) and integration of the distinctive low-MW peak (nonextended chains; MW < ~36 000 g/mol) relative to the overall distribution revealed a degree of livingness of ~71%. The polymerization with the highest $R_p$ ($d_n \approx 70$ nm; 92% conversion sample) resulted in essentially all chains being dead, as revealed by the completely unsuccessful chain extension in Figure 2b.

Extensive discussion of experimental results of TEMPO-mediated radical polymerization of S in aqueous miniemulsion published to date has recently been provided elsewhere.[30,33] In short, previous experimental work has in the vast majority of cases indicated great similarity with the corresponding bulk system.[17,19,20,22−24,26] However, it is believed that this is as a result of the particles having been too large for compartmentalization[33,34] and interface[30] effects to be significant. (Even if $d_n$ is low, a broad particle size distribution, as is often the case in miniemulsions, will mean most polymer is formed in the larger particles.[20])

**Confirmation of Nucleation Mechanism Using Fluorescence Analysis.** Considering that $R_p$ was extremely high in the miniemulsion with the smallest particle size ($d_n \approx 70$ nm; Figure 1), an issue of concern is whether monomer droplet nucleation according to the generally accepted mechanism in miniemulsion polymerization[42] is the only significant mode of nucleation or whether secondary nucleation may be occurring to some extent. On the basis of the data at hand (in particular, the nonliving nature of the MWDs for the smallest particles[30]), one might envisage that secondary nucleation may occur, thus leading to some conventional (nonliving) polymerization in these secondary particles (because they would contain an insufficient amount of nitroxide).

To this end, miniemulsion polymerizations were carried out using a PS-TEMPO macroinitiator labeled with a small amount of the FL monomer 1-pyrenylmethyl methacrylate ($PS_{FL}$-TEMPO), using the same recipe and emulsification technique as the miniemulsion with $d_n \approx 70$ nm in Figure 1. Because of the hydrophobicity of the $PS_{FL}$-TEMPO macroinitiator, any polymer formed as a result of secondary nucleation would not contain any segment originating from $PS_{FL}$-TEMPO, and thus it is possible to differentiate between polymer initiated by $PS_{FL}$-TEMPO (i.e., in the monomer droplets) and polymer formed by secondary nucleation by comparison of MWDs obtained from the RI and FL detectors in the GPC analysis.

The particle size, the conversion−time data, and the MWD in the polymerization using $PS_{FL}$-TEMPO were essentially the same as those of the polymerization with $d_n \approx 70$ nm in Figure 1. Figure 3 shows an overlay of the MWDs derived from RI and FL detection (see Experimental Section for details) at 65% conversion (15 min), revealing that the two MWDs were close to identical. The very vast majority of chains have thus been initiated by $PS_{FL}$-TEMPO; i.e., secondary nucleation plays a negligible role in the polymerization.

**Compartmentalization.** Compartmentalization in NMP[33,34,43,44] (and ATRP[35]) in dispersed systems manifests itself as segregation effects and confined space effects. For S/TEMPO/125 °C with $[PS\text{-}TEMPO]_0 = 0.02$ M, $d < 70$ nm is required for compartmentalization effects to become important.[33,34] The main effect of compartmentalization in the present system (i.e., for $d < 70$ nm) would be an increase in the deactivation rate as a result of the confined space effect,[33,34] the overall result being a reduction in $R_p$. In the present system, a very significant increase in $R_p$ was observed for the miniemulsion with $d_n \approx 70$ nm, and it can be concluded that compartmentalization effects are not likely to be important, as expected, in the present system.

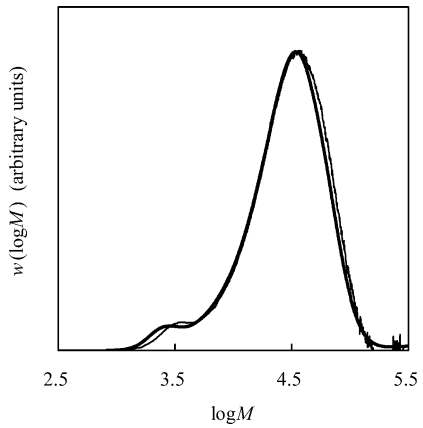


**Figure 3.** Molecular weight distributions (normalized to peak height) derived from RI (thick line) and FL detection (thin line) at 65% conversion in TEMPO-mediated miniemulsion polymerizations of S with 8 wt % SDBS and 8 wt % hexadecane (relative to S) using a fluorescence-labeled macroinitiator ($[PS_{FL}\text{-}TEMPO]_0 = 0.02$ M) at 125 °C ($d_n \approx 70$ nm).

Very recently, Maehata et al.[45] reported data on the TEMPO-mediated polymerization of S in miniemulsion at 135 °C using the surfactant DOWFAX 8390. As $d_w$ decreased from 180 to 50 nm with increasing surfactant concentration, $R_p$ decreased and the livingness increased, but $M_w/M_n$ remained relatively unaffected. $R_p$ in miniemulsion was lower than in bulk, but the bulk system exhibited intermediate livingness (i.e., not the lowest livingness as predicted by compartmentalization effects only). These results (with the exception of the livingness in the bulk system) are consistent with compartmentalization effects. More specifically, the confined space effect on deactivation and geminate termination of thermal radicals generated in pairs (thermal initiation of S) results in lower $R_p$ for small particles, and segregation of propagating radicals results in improved livingness.[33,34] On the basis of the $d_w$ values reported, the particle sizes in the work by Maehata et al. are smaller than in the present study ($d_w = 50-180$ nm, to be compared with $d_w = 90-220$ nm (main data set in Figure 1)). It is speculated that for sufficiently small particles the confined space effect outweighs the interface effect. Very recent work on TEMPO-mediated polymerization of S in microemulsion also supports this notion.[46] However, as discussed below (in the section Simulations and Mechanistic Discussion), it is also likely that the absence of SDBS in Maehata's work contributed to the absence of rate enhancement for small particles. Moreover, hexadecane was employed in the present study (to suppress Oswald ripening), but not in the work of Maehata et al.

**Nitroxide Partitioning**. Nitroxide partitioning to the aqueous phase may influence miniemulsion NMP.[8,9,21,32] In order to experimentally confirm the absence of significant nitroxide partitioning effects, a macroinitiator based on polymeric TEMPO (Scheme 1) was employed. The polymeric segment renders this nitroxide sufficiently hydrophobic for partitioning to the aqueous phase to be negligible. Prior to the miniemulsion polymerization, the polymeric TEMPO macroinitiator was confirmed to behave without abnormalities in the corresponding bulk polymerization (see Experimental Section).

The conversion−time data in Figure 1 ($d_n \approx 62$ nm) reveal that $R_p$ was very high also using polymeric TEMPO, and thus one can conclude that nitroxide partitioning is not an important factor with regards to $R_p$ in the present systems. The corresponding MWDs were bimodal at all conversions and displayed essentially no signs of control/livingness (Figure 4). The peak at low MW at 39% conversion largely corresponds to macro-

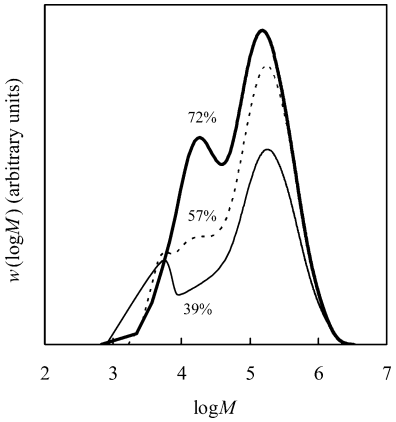


**Figure 4.** Molecular weight distributions at different conversions as indicated in "polymeric TEMPO"-mediated miniemulsion ($d_n \approx 62$ nm, $d_w \approx 76$ nm) polymerization of S ([macroinitiator]$_0 = 0.02$ M) with 8 wt % SDBS and 8 wt % hexadecane (relative to S) at 125 °C. The GPC distributions ($w(\log M)$) correspond to normalized weight distributions (relative to conversion, considering the mass of the initial macroinitiator), i.e., direct comparison of the distributions is possible.

initiator that has not yet partaken in significant propagation. As conversion increased, a bimodal distribution formed, with little change in the MWD with conversion. This behavior was similar to that observed in the polymerization with $d_n \approx 70$ nm and PS-TEMPO, although in the latter polymerization a monomodal MWD was obtained (not counting the low MW corresponding to PS-TEMPO).

The experimental finding that nitroxide partitioning has little effect on these polymerizations is in agreement with theory. In the absence of compartmentalization effects[33,34,43] (i.e., for sufficiently large particles) and assuming phase transfer equilibrium,[47] nitroxide partitioning only affects the polymerization in the prestationary state[32] (the same principles apply to ATRP in dispersed systems[48]). In the prestationary state, increased nitroxide partitioning to the aqueous phase leads to a higher concentration of propagating radicals in the organic phase and thus higher $R_p$ and more termination (lower livingness). However, as more nitroxide is released as a result of termination, the nitroxide concentrations in both the organic and aqueous phases keep increasing until the concentration in the organic phase is the same as in the corresponding bulk system at the stationary state. The net effect of partitioning is thus that in the prestationary state more termination is required to occur to release enough nitroxide to reach the stationary state organic phase concentration because of loss of nitroxide to the aqueous phase. However, once the stationary state has been reached, the polymerization proceeds exactly as it would in the absence of partitioning. The stationary state is reached within minutes for S/TEMPO/125 °C in bulk.[2] Simulations[32] based on the partitioning coefficient of TEMPO between S and water ($[\text{TEMPO}]_S/[\text{TEMPO}]_{aq} = 98.8$ at 135 °C[47,49]) have shown that partitioning results in an increase in the propagating radical concentration of less than a factor of 2 for the first 5 min of the polymerization, consistent with the experimental findings that partitioning has a negligible effect on the present polymerization system. It is not clear why $R_p$ was greater for TEMPO than polymeric TEMPO at conversions beyond ~50% (Figure 1), although this is not believed to be related to nitroxide partitioning.

**Addition of Free TEMPO**. Free TEMPO was added to the miniemulsion NMP system for two reasons: (i) to examine whether this would increase the control/livingness for small particles and (ii) to gain mechanistic understanding.

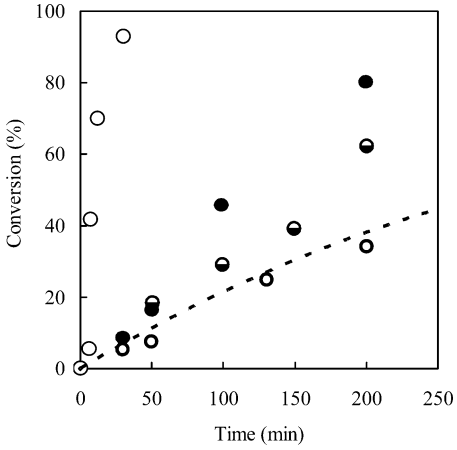


**Figure 5.** Conversion−time data for TEMPO-mediated miniemulsion polymerizations of S with [PS-TEMPO]$_0 = 0.02$ M at 125 °C in the presence of 2 (●, $d_n \approx 80$ nm), 5 (◒, $d_n \approx 74$ nm), and 20 mol % (open circles with thick lines, $d_n \approx 73$ nm) free TEMPO (relative to PS-TEMPO). The fastest polymerization from Figure 1 (○, $d_n = 70$ nm, no free TEMPO) is included for comparison. All polymerizations contained 8 wt % SDBS and 8 wt % hexadecane (relative to S). The broken line is bulk at 125 °C from ref 52.

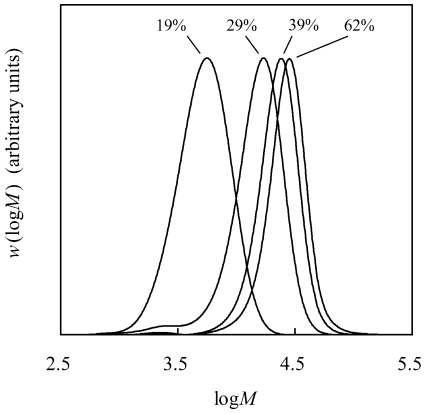


**Figure 6.** Molecular weight distributions (normalized to peak height) at different conversions as indicated in the TEMPO-mediated miniemulsion polymerizations of S with [PS-TEMPO]$_0 = 0.02$ M and 8 wt % SDBS and 8 wt % hexadecane (rel. to S) at 125 °C in the presence of 5 mol % free TEMPO (relative to PS-TEMPO) ($d_n \approx 74$ nm).

Figure 5 shows conversion−time data for TEMPO-mediated polymerization of S in aqueous miniemulsion at 125 °C with PS-TEMPO and 2 ($d_n \approx 80$ nm), 5 ($d_n \approx 74$ nm), and 20 mol % ($d_n \approx 73$ nm) free TEMPO (relative to [PS-TEMPO]$_0$). $R_p$ decreased significantly on addition of TEMPO; the miniemulsion system containing 20% free TEMPO polymerized with a rate similar to the bulk system in the absence of free TEMPO. The miniemulsion polymerizations with 2 and 5% free TEMPO were slower than the corresponding miniemulsion system without free TEMPO but faster than the bulk system without free TEMPO. As anticipated, the addition of free TEMPO led to an increase in control/livingness. Figure 6 shows MWDs at different conversions obtained in the presence of 5 mol % free TEMPO, revealing how the control/livingness was good, with $M_w/M_n = 1.22$ at 62% conversion, despite $R_p$ being significantly greater than in the bulk system. Thus, the present approach may offer a way of increasing $R_p$ in TEMPO-mediated polymerizations while still maintaining a reasonable level of control/livingness.

In order to analyze the effect of addition of TEMPO on $R_p$ in a more quantitative manner, simulations using the software PREDICI[38] of the corresponding bulk polymerization of S in the presence of various amounts of free TEMPO were carried

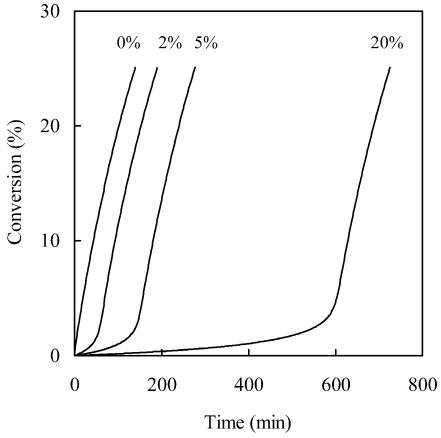


**Figure 7.** Simulated conversion−time data (eqs 1−4) for TEMPO-mediated bulk polymerization of S at 125 °C with PS-TEMPO in the presence of various amounts of free TEMPO (percentages indicate initial mol % free TEMPO relative to PS-TEMPO; $[PS\text{-}TEMPO]_0 = 0.02$ M).

out based on the generally accepted mechanism in a homogeneous system according to eqs 1−4:[2]

$$\frac{d[M]}{dt} = -k_p[P^\bullet][M] \quad (1)$$

$$\frac{d[PT]}{dt} = k_c[P^\bullet][T^\bullet] - k_d[PT] \quad (2)$$

$$\frac{d[P^\bullet]}{dt} = k_d[PT] - k_c[P^\bullet][T^\bullet] - 2k_t[P^\bullet]^2 + k_{i,th}[M]^3 \quad (3)$$

$$\frac{d[T^\bullet]}{dt} = k_d[PT] - k_c[P^\bullet][T^\bullet] \quad (4)$$

where M, PT, P$^\bullet$, and T$^\bullet$ denote monomer, alkoxyamine (living chains), propagating radicals, and nitroxide, respectively, and $k_p$ ($2.32 \times 10^3$ $M^{-1}$ $s^{-1}$ [50]), $k_c$ ($7.6 \times 10^7$ $M^{-1}$ $s^{-1}$ [51,52]), $k_d$ ($1.6 \times 10^{-3}$ $s^{-1}$ [51]), $k_t$ ($1.72 \times 10^8$ $M^{-1}$ $s^{-1}$ [53]), and $k_{i,th}$ ($1.70 \times 10^{-10}$ $M^{-2}$ $s^{-1}$ [54]) are the rate coefficients for propagation, coupling (deactivation), alkoxyamine dissociation (activation), bimolecular termination, and thermal (spontaneous) initiation of S, respectively, with initial concentrations $[PT]_0 = 0.02$ M and $[M]_0 = 8.73$ M. The simulations were only taken to 25% monomer conversion, thus justifying the use of conversion-independent values of $k_p$, $k_t$, and $k_c$.[55] Equations 1−4 are the chain-length-independent versions of the actual equations that PREDICI solves, which are based on each individual chain length. PREDICI keeps track of the individual molecular weight distributions of propagating radicals, dormant chains (PT), and dead chains, and the degree of livingness (the number fraction of dormant chains) can readily be calculated from simulated data (see below).

Simulated conversion−time profiles (Figure 7) reveal that 2, 5, and 20 mol % free TEMPO result in very significant inhibition, the extent of which increases with increasing amount of free TEMPO. After the inhibition, the polymerizations proceed with the same $R_p$ as in the absence of free TEMPO, regardless of the initial amount of TEMPO. These simulations are in agreement with previous experimental work[56] and current mechanistic understanding.[2] During the inhibition period, TEMPO is gradually consumed by radicals generated by thermal initiation[54] of S. (Thermal radicals may add to S prior to reaction with TEMPO depending on the TEMPO concentration.[57])

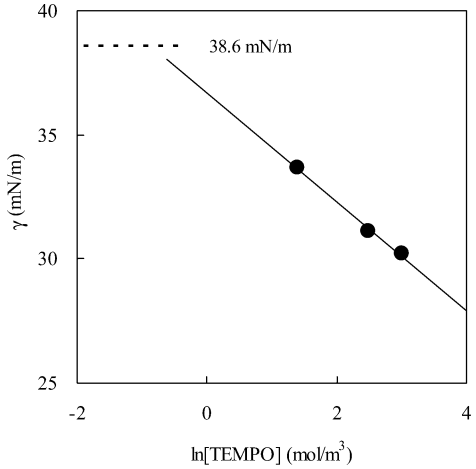


**Figure 8.** Interfacial tension between styrene/*n*-hexadecane (100/8, w/w) containing dissolved TEMPO and water as a function of TEMPO concentration measured by the pendant drop method.

No inhibition was observed in the experimental miniemulsion systems, despite the presence of as much as 20 mol % free TEMPO (Figure 5). Moreover, $R_p$ decreased with increasing amount of free TEMPO (unlike in the simulated bulk system, where $R_p$ is unaffected by the initial amount of free TEMPO after the inhibition). Thus, the experimental and simulated results using free TEMPO provide further evidence that the miniemulsion polymerizations proceeded very differently from the corresponding bulk system.

Pan et al.[58] did observe induction periods on addition of free TEMPO to thermal miniemulsion polymerizations of S (i.e., no added initiator or PS-TEMPO) at 125 °C using the surfactant Dowfax 8390 (disulfonated alkyldiphenyl oxide sodium salt), and $R_p$ after the induction period was not significantly affected by the initial amount of TEMPO. However, no information on particle size was given in that work.

**Interface Effect.** We have previously proposed that an interface effect is operative in the present miniemulsion polymerizations, whereby the effective TEMPO concentration in the particles is reduced due to a significant fraction of TEMPO being located in the vicinity of and/or adsorbed at the interface between the aqueous and the organic phases.[30] Some fraction of the nitroxide would thus be unable to participate in the NMP mechanism (i.e., the deactivation reaction), and the significance of this effect would increase with decreasing particle size (increasing total interfacial area).

The interfacial tension between water and S/hexadecane (100/8, w/w) containing various amounts of TEMPO was measured by the pendant drop method. The interfacial tension decreased with increasing TEMPO concentration, consistent with TEMPO being surface active and some fraction of TEMPO being located at the interface (Figure 8). The maximum surface excess concentration ($\Gamma_{max}$) was calculated from the data using Gibbs' adsorption isotherm:[59]

$$\Gamma_{max} = \frac{-1}{RT}\left(\frac{\partial\gamma}{\partial \ln[TEMPO]}\right)_T \quad (5)$$

where $R$ is the gas constant (8.314 J $K^{-1}$ $mol^{-1}$) and $T$ is the temperature (298 K), resulting in $\Gamma_{max} = 8.9 \times 10^{-9}$ mol $dm^{-2}$. The minimum area per TEMPO molecule ($A_{min}$) was subsequently calculated from eq 6:

$$A_{min} = (\Gamma_{max} N_A)^{-1} \quad (6)$$

where $N_A$ is Avogadro's number, giving $A_{min} = 1.87$ nm$^2$. This is similar to what has been obtained for aqueous solutions of sodium dodecyl sulfate (SDS) at the air−liquid interface.[60] For a miniemulsion polymerization with $d_n \approx 110$ nm, this maximum adsorption corresponds to [TEMPO] = 0.19 M (i.e., at full surface coverage, complete desorption would result in [TEMPO] = 0.19 M in the particle). In other words, the interface of a particle with $d_n \approx 110$ nm has more than sufficient "capacity" to adsorb all the free TEMPO available during a TEMPO-mediated polymerization (where [TEMPO] ≪ 0.19 M). The interfacial tensions in Figure 8 do not correspond to the interfacial tensions between the particle phase and the aqueous phase in the actual miniemulsion system due to the presence of the surfactant (which lowers the interfacial tension).

It has previously been reported that the presence of TEMPO results in a reduction in the interfacial tension between dodecane and water.[61] The notion of an interface effect finds further support in electron spin resonance (EPR)[62−64] and optical absorption spectroscopy[65] studies indicating that the nitroxide group (NO•) of various nitroxides tends to be located at the interface in latex particles[62,63] and micelles.[62−65] On the basis of the literature,[62−64] it appears possible (although most likely experimentally challenging) to exploit EPR to gain quantitative information on the distribution of TEMPO (and other nitroxides) between the interior of a latex particle and the interface.

**Simulations and Mechanistic Discussion.** In order to further test the proposed interface effect quantitatively, simulations were carried out using PREDICI. The simulated conversion−time data and MWDs were subsequently compared with the experimental data. The model comprised eqs 1−4, using the same basic set of values for the rate coefficients as listed above ($[S]_0$ = 7.64 M). The simulations were only taken to ∼40% conversion, and thus conversion-independent values of $k_p$, $k_t$, and $k_c$ could be employed.[55] In order for this modeling exercise to be meaningful, it is essential that the model is able to reproduce the conversion−time data in the corresponding bulk polymerization. Even though relatively reliable literature values are available for the required rate coefficients, perfect agreement between model and experiment cannot be expected due to accumulated error in the rate coefficients and chain-length dependence of rate coefficients (mainly $k_t$[66]). The accuracy of the literature value of $k_{i,th}$ is also compromised by assumptions in the model employed by Hui and Hamielec[54] when fitting their experimental data to obtain $k_{i,th}$. In the present study, the model (eqs 1−4) was fitted to the bulk conversion−time data in Figure 1 using $k_{i,th}$ as an adjustable parameter, resulting in $k_{i,th} = 5.4 \times 10^{-10}$ M$^{-2}$ s$^{-1}$. This value is higher than that reported by Hui and Hamielec ($1.70 \times 10^{-10}$ M$^{-2}$ s$^{-1}$).[54]

If an interface effect is operative as outlined above, then the effective TEMPO concentration would be reduced due to some fraction of TEMPO being located at or in the immediate vicinity of the interface, resulting in a reduced deactivation rate. This scenario was modeled by reducing the value of the deactivation rate coefficient ($k_c$) to $k_c'$, which is equivalent to assuming that a constant mol % of the total amount of free TEMPO is adsorbed at (or located near) the interface in such a fashion that it is unable to react with propagating radicals. The mol % free TEMPO adsorbed at the interface is then equal to $100(1 - k_c'/k_c)$. Relatively good agreement between model and experiment in terms of $R_p$ was obtained using $k_c' = 0$ ($d_n \approx 70$ nm) and $1.5 \times 10^5$ M$^{-1}$ s$^{-1}$ ($d_n \approx 110$ nm) (Figure 9). This would correspond to 100% ($d_n \approx 70$ nm) and 99.8% of free TEMPO being adsorbed at the interface, respectively. There was also relatively good agreement (although by no means perfect) between the simulated and experimental MWDs (Figure 10). In particular, the very good agreement between the positions of the MWD peak tops in both cases is noteworthy. The presence of the unreacted PS-TEMPO macroinitiator even at relatively high conversion was reproduced by the model (the low-MW peak in Figure 10b). The chain extension indicated the livingness was close to zero in the fastest polymerization ($d_n \approx 70$ nm; Figure 2b) at 92% conversion, which is in agreement with the simulations. ($k_c = 0$ means the livingness is zero when the initial macroinitiator has dissociated.) Under such a scenario, PS-TEMPO simply acts as a radical initiator, each dissociation event providing one macroradical. The polymerization with $d_n \approx 110$ nm was determined to have a livingness of ∼71% at 79% conversion by chain extension (Figure 2a), which is not inconsistent with the simulations yielding 86% livingness at 37% conversion. (The livingness decreases with increasing conversion.)

If it is assumed that the NMP equilibrium equation (eq 7) is satisfied (theoretical work indicates that this is the case for $d_n$

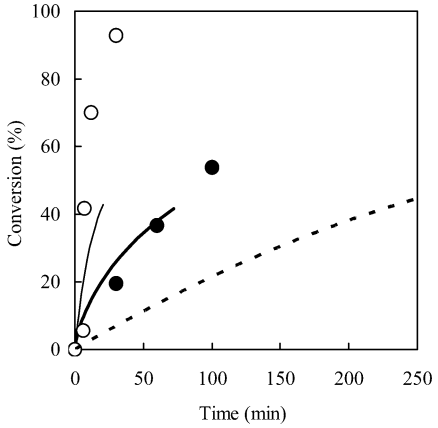


**Figure 9.** Experimental (○; $d_n = 70$ nm; ●; $d_n = 110$ nm; from Figure 1) and simulated (full lines; eqs 1−4) conversion−time data for TEMPO-mediated miniemulsion polymerizations of S ($[PS\text{-}TEMPO]_0$ = 0.02 M) with 8 wt % SDBS and 8 wt % hexadecane (relative to S) at 125 °C. The simulations were carried out with reduced deactivation rates according to $k_c' = 0$ (thin line) and $1.5 \times 10^5$ M$^{-1}$ s$^{-1}$ (thick line) (see text for details). The broken line is bulk at 125 °C from ref 52.

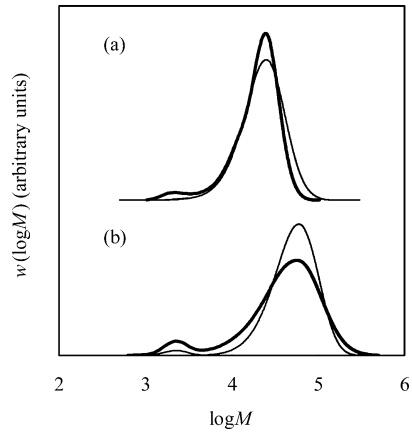


**Figure 10.** Experimental (thick lines) and simulated (thin lines; eqs 1−4) molecular weight distributions of TEMPO-mediated miniemulsion polymerizations of S ($[PS\text{-}TEMPO]_0$ = 0.02 M) with 8 wt % SDBS and 8 wt % hexadecane (relative to S) at 125 °C; (a) $d_n \approx 110$ nm, conversion = 37%; (b) $d_n \approx 70$ nm, conversion = 42%. The simulations were carried out with reduced deactivation rates according to $k_c' = 1.5 \times 10^5$ (a) and 0 M$^{-1}$ s$^{-1}$ (b) (see text for details). The GPC distributions ($w(\log M)$) correspond to normalized weight distributions (relative to conversion, considering the mass of the initial macroinitiator), i.e., direct comparison of the distributions is possible.

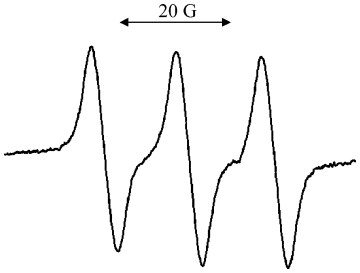


**Figure 11.** EPR spectrum recorded of particle phase (organic phase) of TEMPO-mediated miniemulsion polymerization of S using PS-TEMPO ($[PS\text{-}TEMPO]_0 = 0.02$ M) as macroinitiator with 8 wt % SDBS and 8 wt % hexadecane (relative to S) at 125 °C at 52% conversion. The spectrum can unambiguously be assigned to free TEMPO.

> 70 nm; for smaller particles, the apparent value of the equilibrium constant $K$ decreases due to the confined space effect causing an increase in the deactivation rate[33]—this would cause [TEMPO] as calculated below to be overestimated, and the conclusion below is thus unaffected), NMP in the stationary state obeys eqs 7 and 8:[2,52]

$$K = \frac{k_d}{k_c} = \frac{[P^\bullet][T^\bullet]}{[PT]} \quad (7)$$

$$\frac{d\alpha}{dt} = k_p[P^\bullet](1-\alpha) \quad (8)$$

where $\alpha$ denotes fractional monomer conversion. Graphical estimation of the rate of conversion from Figure 1 for the polymerization with $d_n \approx 110$ nm at 52% conversion yields $[P^\bullet] \approx 4.1 \times 10^{-8}$ M (based on eq 8), which in turn gives $[T^\bullet] \approx 8.7 \times 10^{-6}$ M (eq 7) based on the values of the rate coefficients listed above and assuming ~85% living chains (consistent with the chain extension in Figure 2a; i.e., $[PT] = 0.02 \times 0.85 = 0.017$ M). This value of $[T^\bullet]$ corresponds to free TEMPO that is available to react with $P^\bullet$; i.e., it is not adsorbed at the interface. The concentration of free TEMPO in the organic phase at 52% conversion (100 min) in the miniemulsion polymerization with $d_n \approx 110$ nm was measured by EPR (see Experimental Section; Figure 11), yielding $[TEMPO] = 1.30 \times 10^{-4}$ M, i.e., a factor of 15 higher than calculated based on eqs 7 and 8. The value obtained by EPR corresponds to the total TEMPO concentration in the organic phase, i.e., TEMPO adsorbed at the interface and TEMPO located inside the particle. These results suggest that 93.3% ($= 100(1 - (8.7 \times 10^{-6}/1.30 \times 10^{-4}))$) of the free TEMPO is adsorbed at the interface, which is not too dissimilar from the figure of 99.8% derived above based on kinetic modeling only with a reduced deactivation rate (i.e., not using the EPR data). The EPR measurement of the concentration of free TEMPO is thus consistent with a significant fraction of TEMPO being unable to partake in deactivation, i.e., consistent with an interface effect as described above.

The lack of inhibition on addition of free TEMPO (Figure 5) is also consistent with the proposed interface effect. If a significant fraction of the added free TEMPO is located at the interface, then the rate of deactivation (i.e., reaction with radicals) would be markedly diminished, and consequently the extent of inhibition would be reduced.

Cunningham and co-workers[37] have recently reported experimental evidence that the surfactant SDBS participates in the generation of radicals during TEMPO-mediated polymerization of S in aqueous miniemulsion at 135 °C, thus providing an additional source of radicals (see Introduction). Before examining this in more detail in connection with the present experimental results, it is important to stress that there was a tradeoff between control/livingness and $R_p$ in the present work (higher $R_p$ being accompanied by a reduction in control/livingness). Cunningham et al. reported that control/livingness was only marginally affected at the higher $R_p$.[36,37] However, the polymerization with the highest $R_p$ in the present study (Figure 1) was in fact markedly faster than the polymerization with the highest $R_p$ reported by Cunningham et al.,[37] and it is possible that for smaller particles (i.e., higher $R_p$) control/livingness would have been adversely affected also in the system of Cunningham and co-workers. Pan et al.[22] carried out TEMPO-mediated miniemulsion polymerizations of S at 125 °C using various concentrations of the surfactant Dowfax 8390 (disulfonated alkyldiphenyl oxide sodium salt), obtaining final volume-average particle diameters in the range 60−150 nm, but no significant effects on the polymerization process were detected. ($R_p$ was similar to the bulk system in all cases.) The same authors reported in an earlier study of the same system that the particle size distributions were indeed relatively broad.[20] In the absence of information on the particle size distributions in ref 22, it is reasonable to assume that they were equally broad, and this may thus (at least partially) explain the absence of any particle size effects in that particular study. Importantly, this explanation is also consistent with the absence of compartmentalization effects in ref 22 (i.e., most particles were too large for compartmentalization to be significant—see Compartmentalization section). Another contributing factor to the lack of particle size effects in ref 22 is that DOWFAX 8390 was employed as surfactant as opposed to SDBS, the latter of which (as discussed above) has been proposed to lead to enhanced radical generation with decreasing particle size.

The rate of spontaneous generation of radicals in S emulsion polymerization (using SDS or sodium dioctyl sulfate (Aerosol MA80) as emulsifiers) at 50 °C for 100 nm diameter particles exceeds that of the corresponding bulk system.[31,67,68] The mechanism remains to be clarified, but radical generation occurs in all three phases (monomer droplets, particles, and the aqueous phase).[69] As such, it cannot be excluded that particle size may influence the rate of such radical generation if the mechanism is related to the interface between the particles and the aqueous phase. The rate of spontaneous styrene emulsion polymerization is suppressed by the addition of an aqueous phase radical trap (Fremy's salt), consistent with radical generation occurring in the aqueous phase and/or on the particle surfaces.[70]

Simulations were carried out to investigate whether the particle size effect on TEMPO-mediated polymerization of S in miniemulsion can be explained by the rate of spontaneous initiation increasing with decreasing particle size, without invoking an interface effect. This was done by employing the literature value for $k_c$ ($7.6 \times 10^7$ $M^{-1}$ $s^{-1}$ [51,52]) but treating $k_{i,th}$ as an adjustable parameter. Enhanced spontaneous radical generation would thus be accounted for by an elevated value of $k_{i,th}$. The conversion−time data of the miniemulsion polymerizations were fitted to the model (eqs 1−4). Good agreement between experimental and simulated conversion−time data was obtained with $k_{i,th} = 6.0 \times 10^{-9}$ ($d_n \approx 110$ nm) and $4.9 \times 10^{-7}$ ($d_n \approx 70$) $M^{-2}$ $s^{-1}$ (simulated data not shown). The simulated MWD for $d_n \approx 110$ nm was in relatively good agreement with the experimental MWD (Figure 12a). However, a major discrepancy between the simulated and experimental MWDs was seen for $d_n \approx 70$ nm (Figure 12b), the simulated MWs being much lower than the experimental. The simulated degrees of livingness were 90.2 ($d_n \approx 110$ nm; 37% conversion) and

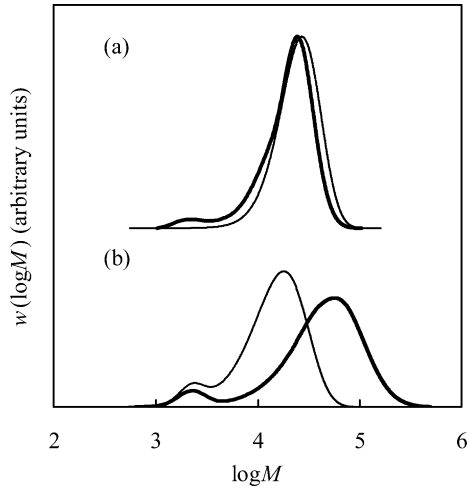


**Figure 12.** Experimental (thick lines) and simulated (thin lines; eqs 1−4) molecular weight distributions of TEMPO-mediated miniemulsion polymerizations of S ([PS-TEMPO]$_0$ = 0.02 M) with 8 wt % SDBS and 8 wt % hexadecane (relative to S) 125 °C; (a) $d_n \approx 110$ nm, conversion = 37%. (b) $d_n \approx 70$ nm, conversion = 42%. The simulations were carried out with enhanced initiation according to $k_{i,th} = 6.0 \times 10^{-9}$ (a) and $4.9 \times 10^{-7}$ M$^{-2}$ s$^{-1}$ (b) (see text for details). The GPC distributions ($w(\log M)$) correspond to normalized weight distributions (relative to conversion, considering the mass of the initial macroinitiator), i.e., direct comparison of the distributions is possible.

49.6% ($d_n \approx 70$ nm; 41% conversion), considerably higher than the experimental estimates of 71 (37% conversion) and 0% (92% conversion), respectively. The model predicts [TEMPO] = $1.42 \times 10^{-5}$ M at 52% conversion ($d_n \approx 110$ nm), which is close to 1 order of magnitude lower than the value obtained by EPR ($1.30 \times 10^{-4}$ M). This is a consequence of the increased radical generation rate leading to a higher rate of consumption of TEMPO. Thus, the information at hand suggests that spontaneous radical generation is most likely playing a significant role in the particle size effects observed in the present study, but this effect cannot alone explain the results.

## Conclusions

The origin of particle size effects in the diameter range of 70−200 nm has been investigated for TEMPO-mediated radical polymerization of S in aqueous miniemulsion with SDBS as surfactant at 125 °C. Extensive experimental and theoretical investigations have been carried out to clarify our earlier reported results that smaller particle size in the diameter range investigated leads to higher $R_p$ but lower control/livingness.[30] The decrease in livingness with decreasing particle size was confirmed by chain extensions. It was confirmed by use of "polymeric TEMPO" that TEMPO partitioning to the aqueous phase has no significant effect on the present results. The results are consistent with an interface effect being operative, whereby some fraction of the free TEMPO is located/adsorbed at the interface, thus reducing the effective TEMPO concentration in the organic phase, which in turn leads to a reduction in the deactivation rate between TEMPO and propagating radicals. This explanation is consistent with experimental results with addition of free TEMPO (no induction period) as well as extensive simulations of the polymerization process using the software PREDICI. Moreover, it was experimentally confirmed that the presence of TEMPO results in a reduction in the interfacial tension between styrene and water, consistent with TEMPO being surface active. However, enhanced (spontaneous) radical generation for smaller particles, possibly related to the presence of SDBS as suggested by Cunningham and coworkers,[36,37] is also likely to play a significant role. Effects of compartmentalization (confined space effect and segregation) are important in nitroxide-mediated radical polymerization of S in dispersed systems but, within the context of the present study, only for particle diameters smaller than ∼70 nm (for [PS-TEMPO] = 0.02 M, as in the present study).[33,34]

The present results offer interesting insight into how one can influence the course of NMP in aqueous dispersed systems by using particle size as an experimental parameter and may as such have practical applications. In the case of styrene/TEMPO, it is possible to obtain a significantly higher polymerization rate while still maintaining reasonable control/livingness by using sufficiently small (but not too small) particles in the presence of an appropriate amount of free TEMPO (for systems initiated by an alkoxyamine). Moreover, it may be possible to exploit the interface effect in TEMPO-mediated polymerization of acrylates, which is severely hampered by excessive buildup of free TEMPO.[71,72] In an acrylate/TEMPO miniemulsion system with sufficiently small particles, the interface effect may lead to a sufficient reduction in the "effective" TEMPO concentration for the polymerization to proceed satisfactorily.

**Acknowledgment.** This work was partially supported by the Support Program for Start-ups from Universities (No. 1509) from the Japan Science and Technology Agency (JST), a Grant-in-Aid for Scientific Research (Grant 17750109) from the Japan Society for the Promotion of Science (JSPS), and a Kobe University Takuetsu-shita Research Project Grant.

## References and Notes

(1) Braunecker, W. A.; Matyjaszewski, K. *Prog. Polym. Sci.* **2007**, *32*, 93−146.
(2) Goto, A.; Fukuda, T. *Prog. Polym. Sci.* **2004**, *29*, 329−385.
(3) Georges, M. K.; Veregin, R. P. N.; Kazmaier, P. M.; Hamer, G. K. *Macromolecules* **1993**, *26*, 2987−2988.
(4) Hawker, C. J.; Bosman, A. W.; Harth, E. *Chem. Rev.* **2001**, *101*, 3661−3688.
(5) Matyjaszewski, K.; Xia, J. *Chem. Rev.* **2001**, *101*, 2921−2990.
(6) Kamigaito, M.; Ando, T.; Sawamoto, M. *Chem. Rev.* **2001**, *101*, 3689.
(7) Moad, G.; Rizzardo, E.; Thang, S. H. *Aust. J. Chem.* **2006**, *59*, 669−692.
(8) Qiu, J.; Charleux, B.; Matyjaszewski, K. *Prog. Polym. Sci.* **2001**, *26*, 2083−2134.
(9) Cunningham, M. F. *Prog. Polym. Sci.* **2002**, *27*, 1039−1067.
(10) Kagawa, Y.; Minami, H.; Okubo, M.; Zhou, J. *Polymer* **2005**, *46*, 1045−1049.
(11) Save, M.; Guillaneuf, Y.; Gilbert, R. G. *Aust. J. Chem.* **2006**, *59*, 693−711.
(12) Marestin, C.; Noel, C.; Guyot, A.; Claverie, J. *Macromolecules* **1998**, *31*, 4041−4044.
(13) Cao, J.; He, J.; Li, C.; Yang, Y. *Polym. J.* **2001**, *33*, 75−80.
(14) Lansalot, M.; Farcet, C.; Charleux, B.; Vairon, J. P.; Pirri, R.; Tordo, P. In *Controlled/Living Radical Polymerization*; Matyjaszewski, K., Ed.; ACS Symposium Series 768; American Chemical Society: Washington, DC, 2000; p 138.
(15) Delaittre, G.; Nicholas, J.; Lefay, C.; Save, M.; Charleux, B. *Chem. Commun.* **2005**, *5*, 614−616.
(16) Delaittre, G.; Nicholas, J.; Lefay, C.; Save, M.; Charleux, B. *Soft Matter* **2006**, *2*, 223−231.
(17) Prodpran, T.; Dimonie, V. L.; Sudol, E. D.; El-Aasser, M. S. *Macromol. Symp.* **2000**, *155*, 1−14.
(18) Farcet, C.; Lansalot, M.; Charleux, B.; Pirri, R.; Vairon, J. P. *Macromolecules* **2000**, *33*, 8559−8570.
(19) Keoshkerian, B.; MacLeod, P. J.; Georges, M. K. *Macromolecules* **2001**, *34*, 3594−3599.
(20) Pan, G.; Sudol, E. D.; Dimonie, V. L.; El-Aasser, M. S. *Macromolecules* **2001**, *34*, 481−488.
(21) Tortosa, K.; Smith, J. A.; Cunningham, M. F. *Macromol. Rapid Commun.* **2001**, *22*, 957−961.
(22) Pan, G.; Sudol, E. D.; Dimonie, V. L.; El-Aasser, M. S. *Macromolecules* **2002**, *35*, 6915−6919.
(23) Cunningham, M. F.; Xie, M.; McAuley, K. B.; Keoshkerian, B.; Georges, M. K. *Macromolecules* **2002**, *35*, 59−66.

(24) Cunningham, M. F.; Tortosa, K.; Ma, J. W.; McAuley, K. B. *Macromol. Symp.* **2002**, *182*, 273−282.
(25) Farcet, C.; Nicolas, J.; Charleux, B. *Macromolecules* **2002**, *40*, 4410−4420.
(26) Cunningham, M.; Lin, M.; Buragina, C.; Milton, S.; Ng, D.; Hsu, C. C.; Keoshkerian, B. *Polymer* **2005**, *46*, 1025−1032.
(27) Zetterlund, P. B.; Alam, Md. N.; Minami, H.; Okubo, M. *Macromol. Rapid Commun.* **2005**, *26*, 955−960.
(28) Cunningham, M. F.; Ng, D. C. T.; Milton, S. G.; Keoshkerian, B. *J. Polym. Sci., Part A: Polym. Chem.* **2006**, *44*, 232−242.
(29) Alam, Md. N.; Zetterlund, P. B.; Okubo, M. *Macromol. Chem. Phys.* **2006**, *207*, 1732−1741.
(30) Nakamura, T.; Zetterlund, P. B.; Okubo, M. *Macromol. Rapid Commun.* **2006**, *27*, 2014−2018.
(31) Gilbert, R. G. *Emulsion Polymerization: A Mechanistic Approach*; Academic Press: London, 1995.
(32) Zetterlund, P. B.; Okubo, M. *Macromol. Theory Simul.* **2005**, *14*, 415−420.
(33) Zetterlund, P. B.; Okubo, M. *Macromolecules* **2006**, *39*, 8959−8967.
(34) Zetterlund, P. B.; Okubo, M. *Macromol. Theory Simul.* **2007**, *16*, 221−226.
(35) Kagawa, Y.; Zetterlund, P. B.; Minami, H.; Okubo, M. *Macromol. Theory Simul.* **2006**, *15*, 608−613.
(36) Cunningham, M. F.; Lin, M.; Keoshkerian, B. *JCT Res.* **2004**, *1*, 33−39.
(37) Lin, M.; Hsu, J. C. C.; Cunningham, M. F. *J. Polym. Sci., Part A: Polym. Chem.* **2006**, *44*, 5974−5986.
(38) Wulkow, M. *Macromol. Theory Simul.* **1996**, *5*, 393−416.
(39) Huan, K.; Bes, L.; Haddleton, D. M.; Khoshdel, E. *J. Polym. Sci., Part A: Polym. Chem.* **2001**, *39*, 1833−1842.
(40) Gilbert, R. G. *Trends Polym. Sci.* **1995**, *3*, 222−226.
(41) Zetterlund, P. B.; Saka, Y.; McHale, R.; Nakamura, T.; Aldabbagh, F.; Okubo, M. *Polymer* **2006**, *47*, 7900−7908.
(42) Asua, J. M. *Prog. Polym. Sci.* **2002**, *27*, 1283−1346.
(43) Tobita, H.; Yanase, F. *Macromol. Theory Simul.* **2007**, *16*, 476−488.
(44) Charleux, B. *Macromolecules* **2000**, *33*, 5358−5365.
(45) Maehata, H.; Buragina, C.; Cunningham, M. *Macromolecules*, in press.
(46) Wakamatsu, J.; Kawasaki, M.; Zetterlund, P. B.; Okubo, M. *Macromol. Rapid Commun.*, in press.
(47) Ma, J. W.; Cunningham, M. F.; McAuley, K. B.; Keoshkerian, B.; Georges, M. K. *Macromol. Theory Simul.* **2002**, *11*, 953−960.
(48) Kagawa, Y.; Zetterlund, P. B.; Minami, H.; Okubo, M. *Macromolecules* **2007**, *40*, 3062−3069.
(49) Ma, J. W.; Cunningham, M. F.; McAuley, K. B.; Keoshkerian, B.; Georges, M. K. *J. Polym. Sci., Part A: Polym. Chem.* **2001**, *39*, 1081−1089.
(50) Buback, M.; Gilbert, R. G.; Hutchinson, R. A.; Klumperman, B.; Kuchta, F. D.; Manders, B. G.; O'Driscoll, K. F.; Russell, G. T.; Schweer, J. *Macromol. Chem. Phys.* **1995**, *196*, 3267−3280.
(51) Goto, A.; Terauchi, T.; Fukuda, T.; Miyamoto, T. *Macromol. Rapid Commun.* **1997**, *18*, 673−681.
(52) Fukuda, T.; Terauchi, T.; Goto, A.; Ohno, K.; Tsujii, Y.; Miyamoto, T.; Kobatake, S.; Yamada, B. *Macromolecules* **1996**, *29*, 6393−6398.
(53) Buback, M.; Kowollik, C.; Kurz, C.; Wahl, A. *Macromol. Chem. Phys.* **2000**, *201*, 464−469.
(54) Hui, A. W.; Hamielec, A. E. *J. Appl. Polym. Sci.* **1972**, *16*, 749−769.
(55) Zetterlund, P. B.; Yamauchi, S.; Yamada, B. *Macromol. Chem. Phys.* **2004**, *205*, 778−785.
(56) Veregin, R. P. N.; Odell, P. G.; Michalak, L. M.; Georges, M. K. *Macromolecules* **1996**, *29*, 2746−2754.
(57) Zetterlund, P. B.; Busfield, W. K.; Jenkins, I. D. *Macromolecules* **2002**, *35*, 7232−7237.
(58) Pan, G.; Sudol, E. D.; Dimonie, V. L.; El-Aasser, M. S. *J. Polym. Sci., Part A: Polym. Chem.* **2004**, *42*, 4921−4932.
(59) Rosen, M. J.; Cohen, A. W.; Dahanayake, M.; Hua, X. *J. Phys. Chem.* **1982**, *86*, 541−545.
(60) Landfester, K.; Bechthold, N.; Tiarks, F.; Antonietti, M. *Macromolecules* **1999**, *32*, 5222−5228.
(61) Pyter, R. A.; Ramachandran, C.; Mukerjee, P. *J. Phys. Chem.* **1982**, *86*, 3206−3210.
(62) Baglioni, P.; Cocciaro, R.; Dei, L. *J. Phys. Chem.* **1987**, *91*, 4020−4023.
(63) Zhou, J.; Chen, S.; Duan, H.; Jiang, M.; Zhang, Y. *Langmuir* **2001**, *17*, 5685−5687.
(64) Weber, S.; Wolff, T.; Bunau, G. v. *J. Colloid Interface Sci.* **1996**, *184*, 163−169.
(65) Ramachandran, C.; Pyter, R. A.; Mukerjee, P. *J. Phys. Chem.* **1982**, *86*, 3198−3205.
(66) Smith, G. B.; Russell, G. T.; Heuts, J. P. A. *Macromol. Theory Simul.* **2003**, *12*, 299−314.
(67) Hawkett, B. S.; Napper, D. H.; Gilbert, R. G. *J. Chem. Soc., Faraday Trans. 1* **1980**, *76*, 1323−1343.
(68) Lansdowne, S. W.; Gilbert, R. G.; Napper, D. H.; Sangster, D. F. *J. Chem. Soc., Faraday Trans. 1* **1980**, *76*, 1344−1355.
(69) Christie, D. I.; Gilbert, R. G.; Congalidis, J. P.; Richards, J. R.; McMinn, J. H. *Macromolecules* **2001**, *34*, 5158−5168.
(70) Lacik, I.; Casey, B. S.; Sangster, D. F.; Gilbert, R. G.; Napper, D. H. *Macromolecules* **1992**, *25*, 4065−4072.
(71) Georges, M. K.; Lukkarila, J. L.; Szkurhan, A. R. *Macromolecules* **2004**, *37*, 1297−1303.
(72) Debuigne, A.; Radhakrishnan, T.; Georges, M. K. *Macromolecules* **2006**, *39*, 5359−5363.

MA0712403